

Raman Longitudinal Acoustic Mode Studies of a Poly(ethylene oxide) Fraction during Isothermal Crystallization from the Melt

Insun Kim[†] and Samuel Krimm*

Macromolecular Science and Engineering Center and Department of Physics, University of Michigan, Ann Arbor, Michigan 48109

Received February 29, 1996; Revised Manuscript Received July 2, 1996[®]

ABSTRACT: Raman longitudinal acoustic mode (LAM) spectra have been obtained during isothermal crystallization from the melt at various temperatures of a poly(ethylene oxide) (PEO) fraction of molecular weight about 3000. At all temperatures, we find an initial single well-defined LAM band corresponding to a helical chain length that represents a non-integral-fold (NIF) structure. With time, and more rapidly at higher crystallization temperatures, the NIF chains transform into integer-fold (IF) structures. The final morphology consists of IF mixed crystals composed mainly of extended (E) chains but with once-folded (F2) chains embedded in them. This solid-state transformation from the NIF state may proceed through the F2 state.

Introduction

When long-chain polymer molecules crystallize from the melt or solution, the molecules tend to form folded chains due to the kinetic origin of crystallization. Such folded structures make it possible for the molecules to be arranged within a lamella of a thickness much smaller than the chain length.¹ Chain folding parameters are affected by the degree of supercooling (or the crystallization temperature, T_c), pressure, and crystallization time (t_c).²

Of particular interest is the chain folding of relatively simple systems such as low molecular weight polymer fractions with no or small polydispersity. Although this may represent a simple system when compared to polydisperse high molecular weight polymer, the crystallization of the fraction can provide clear information on the crystalline morphology. Such crystals generally have simple integer-fold (IF) chain structures, in which case the lamellar thickness is expected to be close to an integral fraction of the extended chain length. The chain ends would then be at the lamellar surfaces and the fold would be sharp with adjacent re-entry.

Low molecular weight poly(ethylene oxide) (PEO) fractions are known to form IF structures. As observed in small-angle X-ray scattering (SAXS) studies by Spegel and co-workers,^{3,4} the PEO molecules were reported to undergo a stepwise transition with a quantized increase in lamellar thickness with crystallization temperature. Such a stepwise transition in PEO crystals has also been observed by studies of crystal growth rate using optical microscopy⁵ and by differential scanning calorimetry (DSC) studies.⁶ These observations confirm the tendency of PEO chains to form IF structures, which allow defects due to the chain ends to be rejected from the crystalline lattice and permit hydrogen bonds to form between end groups in the surface layers of adjacent lamellae.

The longitudinal acoustic mode (LAM) of polymers has been used to study polymer structure and morphology through this skeletal vibration of the crystalline stems within a lamella. For solid *n*-paraffins, LAM vibrations were observed by Mizushima and Simanouti⁷

and the LAM frequencies were shown to be related to the stem length essentially by the elastic rod formula:

$$\nu_L = \frac{m(E)}{L_L(\rho)}^{1/2} \quad (1)$$

where E is the elastic modulus, ρ the density, and L_L the stem length. m is an odd integer (we will be concerned with $m = 1$) since Raman activity is associated with a change in polarizability, and even values of m give no such change. Although an approximation, this relation gives important information, in that the LAM frequency is inversely proportional to the stem length undergoing this vibration. Furthermore, the elastic modulus E can be estimated from the slope of the curve of ν_L vs $1/L$ if the density is known. This quantity represents the maximum attainable elastic modulus of a particular polymer, only approached under ideal processing conditions. Subsequent studies^{8,9} showed that longitudinal interactions modify this relation, and these need to be taken into account if an accurate value of E is to be obtained.¹⁰

The LAM of PEO was first observed by Hartley and co-workers¹¹ for melt-crystallized samples of molecular weights from 1000 to 20 000. They assigned the LAM band based on the smooth shift of its frequencies to lower values with increasing molecular weight. The nature of this LAM was comprehensively investigated by Song and Krimm.^{12,13} They demonstrated the importance of lateral interchain interactions on the LAM frequency of helical molecules from normal mode analyses. For planar zigzag chains, the LAM vibration is not significantly affected by the lateral interactions because the atomic displacements are parallel to the chain axis direction. In the LAM vibrations of helical structures the atomic displacements have significant radial components,¹² and therefore ν_L is much more sensitive to lateral interchain interactions, even of the weak van der Waals type. When low-frequency Raman spectroscopy was used in combination with SAXS and DSC, new morphological features were revealed which were not accessible previously.¹⁴ Carefully grown PEO fractions were shown to have single-crystalline character by SAXS and DSC, but from Raman LAM spectroscopy mixed chain morphologies and bilayer structures were evident.

In addition, the LAM can provide information on chain organization within the lamella. It is generally

[†] Current address: Department of Chemical Engineering, University of California, Davis.

[®] Abstract published in *Advance ACS Abstracts*, October 1, 1996.

the case that lamellar thickness from SAXS is larger than crystal stem length from Raman LAM.¹⁵ This is attributable to the disordered fold surface that must be added to the crystalline stem thickness, which together comprise the change in the electron density periodicity measured by SAXS. However, when chains are tilted to the lamellar surface, the Raman LAM stem length can be larger than the lamellar thickness from SAXS. This had been observed for melt-crystallized polyethylene,¹⁶ and we have observed it in PEO.¹⁷

Such LAM stem-length measurements have also led to the characterization of non-integer-fold (NIF) morphologies. In an NIF crystal there are stem lengths that are much smaller than the crystal thickness. Song and Krimm first observed the existence of NIF chains in PEO from Raman and SAXS observations of a room temperature (RT) crystallized PEO 3000 sample.¹⁸ NIF morphologies were also deduced from synchrotron SAXS observations on PEO fractions at various crystallization temperatures.¹⁹

In order to reveal detailed chain arrangements within a lamella, Raman LAM information is essential. So far there has not been any effort to obtain such spectra during crystallization at temperatures higher than RT. In this study, crystallization and structural transitions during isothermal crystallization were observed by in-situ Raman LAM spectroscopy during isothermal crystallization at elevated temperatures in order to disclose initial chain conformations, the details of the structural transition process, and the chain arrangements after a long crystallization time. We focus here on a sample of 3000 nominal molecular weight, PEO 3000.

Experimental Section

The PEO 3000 fraction was purchased from Scientific Polymer Products, Inc. It has a molecular weight (\bar{M}_n) of 3336 with a polydispersity (\bar{M}_w/\bar{M}_n) of 1.10. Its calculated helix axis (extended) chain length, L_M , is 211 Å, based on the crystallographic structure of PEO.²⁰ Some spectra were obtained on a terminally methoxylated PEO, MPEO, of $\bar{M}_n \approx 3000$.

Raman spectra were obtained with a Spex 1403 double monochromator equipped with holographic gratings and a Spectra Physics 165 argon ion laser operated at 514.5 nm. The laser power was maintained at 400–600 mW. In order to reduce stray light from Rayleigh scattering, a Spex 1442 third monochromator was used. With the third monochromator, the spectral range covered is from 3 to 150 cm^{-1} , the low end of which is usually not readily accessible without it. Typical operating conditions for low-frequency spectra were bandwidth = 1.0–1.5 cm^{-1} , scanning increment = 0.1 cm^{-1} , and integration time = 0.5–2 s depending on the sample condition and crystallization habit. Band frequencies could be measured to $\pm 0.1 \text{ cm}^{-1}$.

The spectral information which matters most in this study is the exact peak position to be converted into the crystalline stem length. Calibration of the spectrometer thus becomes very important. For calibration, the pure rotational Raman bands due to air (nitrogen and oxygen) were observed from an empty glass capillary. These bands,²¹ particularly in the range of 20–65 cm^{-1} , were especially useful because of their strong intensities.

Each sample of about 2–3 mg was contained in a thin-walled glass capillary sealed by flame to prevent contamination of the sample. Before sealing, the capillary was flushed with argon gas to eliminate possible air scattering. For the in-situ Raman observation during crystallization, a special sample holder was devised. The holder consists of two chambers whose temperatures are individually controlled by circulating water from precision water baths, the temperatures of both chambers being kept to within $\pm 0.2 \text{ }^\circ\text{C}$. One of the chambers is used for melting or self-seeding of the sample in the glass capillary and the other is for crystallization. The

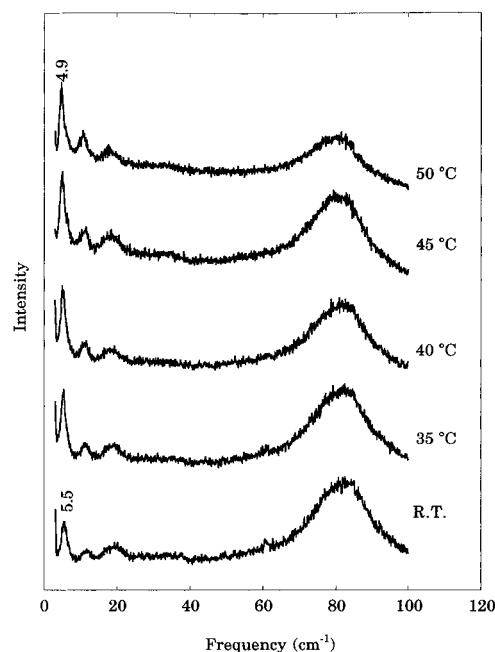


Figure 1. Low-frequency Raman spectra of PEO 3000 ($T_c = 47.0 \text{ }^\circ\text{C}$, $t_c = 5$ days) taken at different temperatures.

sample can be moved rapidly from the melting to the crystallization chamber, which has guide holes for the exciting laser light and the scattered light from the sample.

Temperature Effect on LAM and Its Correction

The effect of temperature on the LAM frequency is crucial when interpreting in-situ Raman observations during crystallization. The usual LAM frequency–chain length calibration curve is based on the crystalline structure and Raman observations at RT, while in-situ Raman observations are made at the crystallization temperatures. Therefore, it can be misleading to interpret the Raman LAM data at T_c higher than RT without knowledge of the temperature effect. For example, ν_L appears at 5.5 cm^{-1} for the extended chain of a well-crystallized PEO 3000 sample which has $L_L = 209 \text{ Å}$ (Figure 1). At 50 $^\circ\text{C}$ the band appears at 4.9 cm^{-1} , which corresponds to a chain length of $L_L = 235 \text{ Å}$ from the frequency–chain length calibration curve. The large frequency decrease is mainly a result of the decrease in interchain interactions that result from the thermal expansion of the unit cell;¹² the stem length itself cannot change this drastically. This expansion is also reflected in the decrease in the frequency of the 19.5 cm^{-1} lattice mode¹⁴ from this value at room temperature to $\sim 18 \text{ cm}^{-1}$ at 50 $^\circ\text{C}$. (Decreases in hydrogen bond strengths at the chain ends with increasing temperature may also contribute to the decrease in ν_L .¹²)

Since LAM vibrations usually have low frequencies, the observed band shape will be affected both by the frequency and by the temperature at which the measurement is made. Although the correction for these effects²² can be large for broad bands, such as, for example, in the case of polyethylene,²³ this correction does not change the LAM peak position significantly when the peak is narrow.²⁴ For PEO 3000, the LAM peaks are narrow and their positions are changed only slightly ($\sim 0.1 \text{ cm}^{-1}$) by this frequency–temperature correction.²⁴ Therefore, it does not account for the large change in ν_L with temperature observed for PEO, which is due primarily to the change in interchain force perturbations.¹²

In this study, the temperature effect on the ν_L of transient structures during crystallization was accounted for by taking a series of Raman spectra of a well-grown IF crystal as a function of temperature (see Figure 1). The frequency shift at a certain temperature was then applied in correcting the ν_L of a transient (NIF) crystal of that fraction at that temperature. For example, when the PEO 3000 fraction was crystallized at 50 °C, a transient LAM band other than the extended (E) or once-folded (F2) appeared. The transient LAM band frequency was corrected by increasing the observed frequency by 0.6 cm⁻¹, since the LAM band of the stable crystal appears 0.6 cm⁻¹ lower at that temperature than at RT. In this way it is possible to correct for the temperature effect in a consistent manner over the temperature range of interest. In what follows, we designate the temperature-corrected Raman LAM chain length by L_L^* .

We note in passing that the intensity changes with temperature (Figure 1) are consistent with our previous normal mode predictions¹² and LAM observations.¹⁴ The Boltzmann factor²² would result in a small increase in the intensity of the E LAM band with increasing temperature, but not enough to account for the observed increase. Most of the latter is due to the weaker end forces as the temperature is raised.¹² The smaller change in intensity of the F2 LAM band is consistent with one of the folded chain ends being perturbed by weaker van der Waals interactions.^{12,14}

LAM Frequency–Chain Length Relation

Since this study is based on Raman LAM observations and the transformation of observed LAM frequencies into corresponding chain lengths, we need to be assured of the validity of the LAM frequency–chain length relation. An important feature of this relation is that, due to the fundamental nature of the LAM vibration, when the chain length goes to infinity, the corresponding LAM frequency should go linearly to zero. Therefore, the calibration line, viz., ν_L vs $1/L$, should go through the origin. For small L , ν_L may deviate from linearity because of the dispersion relation, as observed for *n*-paraffins,²⁵ the extent being dependent on force perturbations on the chain.

The PEO calibration line for polydisperse long-chain molecules is expected to be quite different from that for uniform short-chain oligomers.¹⁴ This is because, whereas regular hydrogen bonds can form between OH chain ends in adjacent lamellae of uniform oligomers, polydispersity can cause irregularity in the lamellar surface and therefore less uniform hydrogen bonding at chain ends and thus weaker end perturbations. In the case that terminal hydrogen bonding is excluded, such as in MPEO, the calibration curve is even different from that of the polydisperse PEOs, because of the still weaker end perturbations.^{12,14}

These relationships are illustrated in Figure 2. The upper solid line is that calculated for end-hydrogen-bonded chains,^{12,14} and it is in good agreement with observed LAM bands of oligo(oxyethylene)s.¹⁴ The lower solid line is that obtained for MPEO, in which end interactions are of the weak van der Waals type: the two high-frequency points are calculated values for oligomers¹² and agree very well with observation;²⁶ the two low-frequency points are observed E and F2 values for an MPEO 3000 sample. The broken line represents the calibration based on observed polydisperse PEO samples.¹⁴ It departs from the MPEO line at small L ,

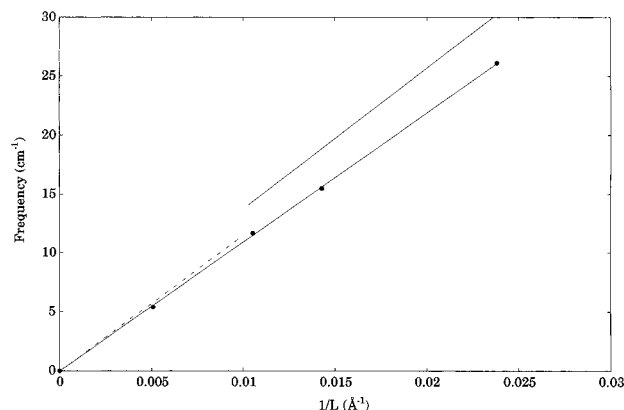


Figure 2. LAM frequency–chain length relation for PEO and MPEO: upper solid line, calculated for oligo(oxyethylene)s;¹⁴ lower solid line, MPEO (see text for description of points); broken line, observed for polydisperse PEOs.

where expected hydrogen bond interactions come into play, and it approaches the MPEO line at large L , where lamellar surface disorder due to polydispersity (or possibly to large-amplitude longitudinal motions²⁷) tends to reduce chain-end interactions. These calibration lines are given by

$$\text{PEO: } \nu_L = 1161.1(1/L_L) \quad (2)$$

$$\text{MPEO: } \nu_L = 1094.7(1/L_L) \quad (3)$$

where ν is in cm⁻¹ and L_L is in Å.

PEO molecules in NIF conformations may not have as regular lamellar surfaces as in the case of IF chains, and their chain ends most likely do not experience axial hydrogen bond forces. Since hydrogen bonding has an important effect on ν_L , this has to be considered when we are dealing with the non-integer-fold. In this study, the PEO and MPEO calibration lines were used selectively depending on the expected chain conformations. For example, for IF chains which have strong chain-end interactions, the PEO calibration line was used to obtain L_L from ν_L . For NIF chains, where a more disordered interlamellar region is expected, the MPEO calibration line was used, although chain length data from the PEO calibration line was also considered in the analysis.

Another aspect of the conversion of ν_L to chain length is the necessity to be certain that the crystalline packing in the monoclinic unit cell of PEO is the same for crystals at the initial and later stages of crystallization. Otherwise, since the LAM of helical chains is sensitive to lateral interchain interactions, a change in unit cell dimension would mean that an NIF LAM frequency could not be translated into a chain length on the same basis as the LAM of a well-crystallized sample.

There are two ways to determine the variation in chain arrangement in a unit cell during crystallization. One is by wide-angle X-ray diffraction (WAXD). A recent publication on a WAXD study during crystallization of PEO²⁸ shows that the crystalline spacings in the initial stages of crystallization stay the same during crystallization. This study finds that only the crystallinity changes during the remaining time of crystallization. In addition, when a quenched and an annealed crystal are compared, WAXD patterns are observed to remain unchanged.

The second method is to examine the lattice vibrations in the low-frequency Raman spectrum itself. Since the

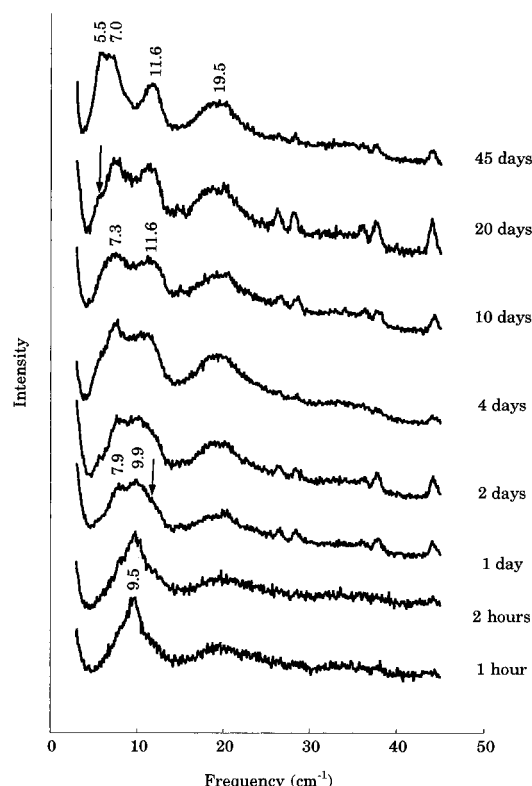


Figure 3. Low-frequency Raman spectra of PEO 3000 during crystallization at T_c = room temperature.

lattice modes represent vibrations in which chains in the unit cell undergo motions with respect to each other, changes in the crystalline arrangement will result in shifts in these frequencies (as occur with temperature). As is clearly seen from the Raman spectra to be presented here (Figures 3–5), there is no change in the lattice mode bands with crystallization time at a given crystallization temperature. This is in agreement with the WAXD observations. Therefore, we can be sure that when the NIF chains first crystallize, they remain in the same arrangement as at later times. This guarantees that our conversion of the LAM frequencies into chain lengths, with a proper temperature correction, is valid at the initial as well as later stages of the crystallization.

Results

Raman LAM spectra were observed as a function of t_c for T_c = RT, 35.0 °C, 38.5 °C, 40.0 °C, 42.0 °C, 43.5 °C, 45.0 °C, 47.0 °C, and 48.5 °C.²⁴ Several of these results are presented here.

For the PEO 3000 fraction, $L_M = 211$ Å, a well-crystallized sample ($T_c = 47.0$ °C and $t_c = 5$ days) gives the RT low-frequency Raman spectrum shown in Figure 1. The spectrum contains several bands in the frequency region below 100 cm^{-1} . There is a sharp band at 5.5 cm^{-1} , which is the ν_L of E chains of $L_L = 209$ Å. Another LAM band appears at 11.6 cm^{-1} , corresponding to F2 chains of $L_L = 99$ Å. Broad bands at 19.5 and near 33 cm^{-1} represent lattice modes,¹⁴ the band near 33 cm^{-1} not being as distinct as the one near 19.5 cm^{-1} . A strong and broad band at 80 cm^{-1} is composed of an overlap of a lattice mode and the CO torsion mode of the PEO chain.^{14,29}

When this fraction crystallizes at RT, the initial LAM band does not correspond to either the E or the F2 chain; it therefore must correspond to an NIF chain (Figure 3

Table 1. Observed Raman LAM Frequencies (cm^{-1}) and Corresponding Chain Stem Lengths (Å) as a Function of Crystallization Time of PEO 3000 at T_c = Room Temperature

t_c	ν_L	L_L	fold ^a
3 min	9.1	120	NIF
1 h	9.5	115	NIF
2 h	9.5	115	NIF
1 day	7.9	139	NIF
	9.9	111	NIF
	11.6 (sh)	99	F2
2 days	7.7	142	NIF
	10.2	107	NIF
10 days	7.3	150	NIF
	11.6	99	F2
20 days	5.5 (sh)	209	E
	7.3	150	NIF
	11.6	99	F2
45 days	5.5	209	E
	7.0	156	NIF
	11.6	99	F2

^a NIF = non-integer-fold, E = extended, F2 = once-folded.

and Table 1). The initial ν_L appears at 9.1 cm^{-1} ($L_L = 120$ Å), which is between the LAM of the E chain (at 5.5 cm^{-1}) and the F2 chain (at 11.6 cm^{-1}), and it shifts to a slightly higher frequency (by about 0.5 cm^{-1}) during the early stages of crystallization. Further shifts take a long time, usually days at this crystallization temperature. With additional crystallization time, the initial LAM band broadens and splits into two bands at $t_c = 1$ day. Of the two bands, the higher frequency band appears to have a shoulder near 11.6 cm^{-1} , where the F2 LAM occurs, and becomes more distinct with crystallization time. At $t_c = 10$ days, the higher frequency band is located at 11.6 cm^{-1} , and further crystallization only shapes up the band more conspicuously without further change in the peak position.

The lower frequency band increases its intensity compared to the higher one with crystallization time, and at $t_c = 20$ days a shoulder appears on the low-frequency side of it. At $t_c = 45$ days, the lower frequency band itself has a doublet character with one peak at 5.5 cm^{-1} and the other at 7.0 cm^{-1} . The peak at 5.5 cm^{-1} represents the E LAM ($L_L = 209$ Å) and the peak at 7.0 cm^{-1} ($L_L = 156$ Å) must result from another NIF structure.

When the crystallization temperature is raised to 35.0 °C. (Figure 4 and Table 2), the initial LAM band appears at a lower frequency, viz., at 8.1 cm^{-1} , than that of the RT crystallization. Without any correction, this frequency corresponds to a $L_L = 135$ Å. When corrected for the temperature effect, $L_L^* = 132$ Å. Thus, the initial chains must also be regarded as NIF chains. With increasing crystallization time, the LAM band changes its shape and peak position. At $t_c = 120$ min, the spectrum clearly shows two low-frequency peaks at 6.3 cm^{-1} ($L_L^* = 168$ Å) and 8.9 cm^{-1} ($L_L^* = 120$ Å). Further crystallization brings up weak but distinctive peaks at 5.3, 6.8, and 11.3 cm^{-1} . The peaks at 5.3 and 11.3 cm^{-1} represent the E and F2 chains, respectively. The peak at 6.8 cm^{-1} ($L_L^* = 156$ Å) represents an NIF LAM band.

Crystallization at 47.0 °C yields the series of spectra shown in Figure 5 (Table 3). At this crystallization temperature, the initial crystallization, nucleation, and deposition of chains on the crystal growth surfaces take a longer time, up to a few minutes, and a large portion of the chains remain in the supercooled melt state. During this period the specimen does not give a good spectrum due to the strong Rayleigh scattering in the

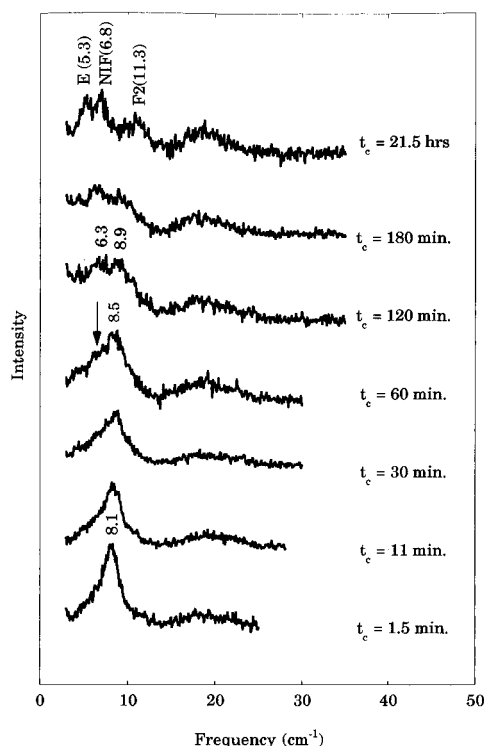


Figure 4. Low-frequency Raman spectra of PEO 3000 during crystallization at $T_c = 35.0$ °C. E represents the extended chain; F2, once-folded; NIF, non-integer-fold.

Table 2. Observed Raman LAM Frequencies (cm^{-1}) and Corresponding Chain Stem Lengths (\AA) as a Function of Crystallization Time of PEO 3000 at $T_c = 35.0$ °C

t_c	ν_L	L_L^{*a}	fold ^b
1.5 min	8.1	132	NIF
11 min	8.1	132	NIF
30 min	8.5	126	NIF
60 min	6.5 (sh)	163	NIF
	8.5	126	NIF
120 min	6.3	168	NIF
	8.9	120	NIF
180 min	6.3	168	NIF
	9.3	115	NIF
21.5 h	5.3	209	E
	6.8	156	NIF
	11.3	100	F2

^a Temperature-corrected L_L . ^b NIF = non-integer-fold, E = extended, F2 = once-folded.

low-frequency region from the supercooled melt. At $t_c = 6.5$ min, the Raman scan first gives a reasonable spectrum. At this stage, the spectrum contains a strong NIF LAM band, at 6.2 cm^{-1} ($L_L^* = 161 \text{ \AA}$), with contributions from the E LAM and F2 LAM bands. As previously observed (Figure 1), at high temperature the lattice modes decrease in relative intensity, and at 47.0 °C the lattice mode at 19.5 cm^{-1} is in fact not as evident as in the Raman spectra of the lower temperature crystallizations. The changes in the LAM bands are obviously fast. In about 40 min, the spectrum closely resembles that of a well-crystallized sample, although there is hint of an NIF band on the high-frequency side of the E LAM band.

Discussion

Our Raman LAM studies of the time course of crystallization in PEO 3000 at different isothermal crystallization temperatures shed light on the chain morphologies in the initial state, on the transformation

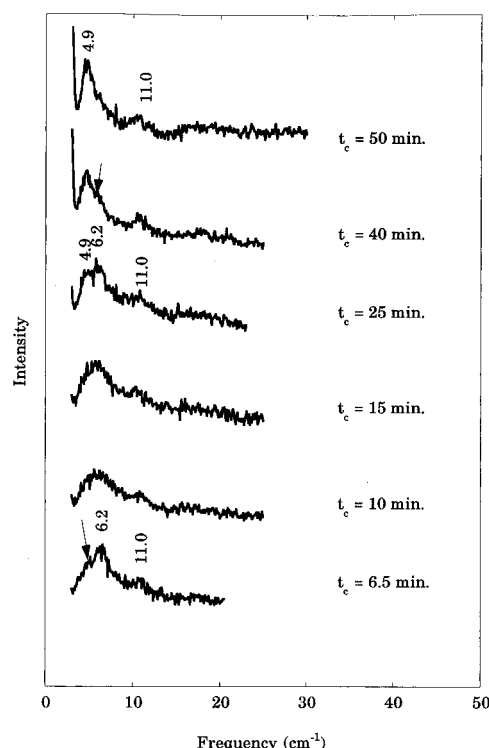


Figure 5. Low-frequency Raman spectra of PEO 3000 during crystallization at $T_c = 47.0$ °C.

Table 3. Observed Raman LAM Frequencies (cm^{-1}) and Corresponding Chain Stem Lengths (\AA) as a Function of Crystallization Time of PEO 3000 at $T_c = 47.0$ °C

t_c	ν_L	L_L^{*a}	fold ^b
6.5 min	5.0 (sh)	206	E
	6.2	161	NIF
	11.0	99	F2
10 min	5.8 ^c		E + NIF
	11.0	99	F2
15 min	5.7 ^c		E + NIF
	11.0	99	F2
25 min	4.9	209	E
	6.2	161	NIF
	11.0	99	F2
40 min	4.9	209	E
	6.0 (sh)	166	NIF
	11.0	99	F2
50 min	4.9	209	E
	11.0	99	F2

^a Temperature-corrected L_L . ^b NIF = non-integer-fold, E = extended, F2 = once-folded. ^c A broad peak at $5.8(7) \text{ cm}^{-1}$ is likely to be an overlap of E and NIF.

process, and on the chain morphologies in the final state.

Morphologies in the Initial State. Several features of the morphological state of the PEO 3000 chains in the initial stages of crystallization stand out. First, the LAM spectra are dominated by an NIF band, as previously noted.^{14,17} This is true even though weak E and F2 bands become evident for higher T_c . Second, the initial NIF bands are well-defined and have half-widths comparable to those of the final E and F2 bands. This shows that the initial NIF chain-length distribution is relatively well-defined and narrow. Since the L_L^* is of the same order as the SAXS spacing³⁰ (even taking into account a chain axis tilt to the lamellar surface¹⁷), this indicates that an initial essentially lamellar-type structure is formed with, because of the intense SAXS scattering,³⁰ a highly disordered surface. Third, the initial NIF chain length increases with T_c , as shown in

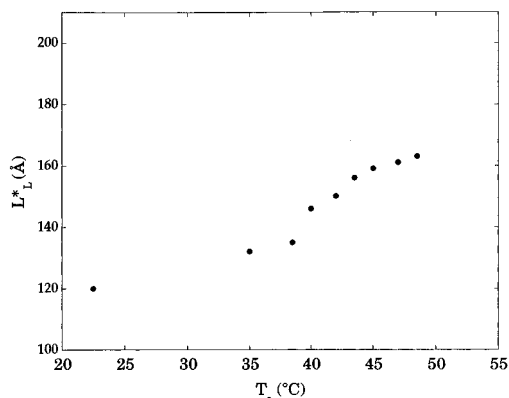


Figure 6. Initial NIF stem length (L_L^*) of PEO 3000 as a function of crystallization temperature. (Initial spectra taken at RT, 3 min; 35.0 °C, 1.5 min; 38.5 °C, 2 min; 40.0 °C, 1 min; 42.0 °C, 3 min; 43.5 °C, 2 min; 45.0 °C, 3 min; 47.0 °C, 6.5 min; and 48.5 °C, 6.75 min.)

Figure 6. This is indicative of a kinetically driven pathway, which in fact has been predicted for PEO by nucleation theory.³¹

These observations suggest certain conclusions. If the initial NIF chain length is well-defined and consistent with a SAXS lamellar thickness, this does not support models in which chains deposit so randomly on the growth faces that the chain length distribution becomes broad, as proposed either for PEO³⁰ or perhaps also for *n*-paraffins.³² The observed narrow distribution, together with the SAXS evidence for a highly disordered surface,³⁰ also suggests that there are essentially no NIF chains that connect adjacent lamellae. The consistent appearance of a minimum near 15 cm⁻¹ and the relatively unchanged lattice mode band near 20 cm⁻¹, regions in which such neighboring-lamellar chain lengths would be expected to appear (given the presence of the dominant NIF L_L^* of ~120–160 Å), support this view. We must elucidate the transformation process from these starting points.

Transformation Process. While we do not know all morphological features of the initially crystallizing state, changes occurring with time as well as the information on the initial state lead to some reasonable inferences. First, if we accept the nonconnectedness of adjacent lamellae, the structural transition from the kinetically favored initial NIF chain structure to the eventual thermodynamically more stable E (plus some F2) chains must be regarded as a chain reorganization that occurs within a lamella in the solid state by motion in the chain axis direction. Whether this takes place by a simple translation or by a "screw" mechanism is not clear at present. Second, for lower T_c there is a tendency for F2 chains to appear before the E chains as crystallization progresses. Even at higher T_c , although E chains appear initially, F2 chains dominate. If NIF chains indeed transform first to F2 chains, possibly with the formation of F2 monolayer lamellae^{17,30} before the conversion to E chains, then this process must be very fast so that both structures form almost simultaneously at high T_c . Of course, we cannot exclude the possibility that, particularly at high T_c , there is a direct NIF → E process accompanying an NIF → F2 → E mechanism.

What is still left unexplained by these results is the detailed structure of the initial state and the mechanics of the transformation. We suppose that the NIF lamellae exhibit significant chain-end disorder, with some ends in the surface layers undoubtedly hydrogen bonded

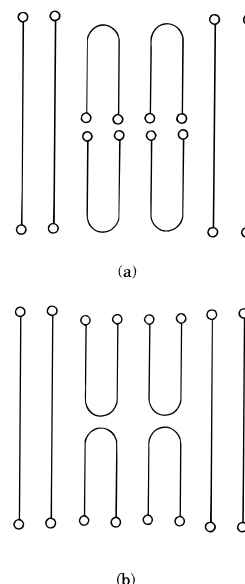


Figure 7. Schematic models of E + F2 crystals: (a) with internal F2 hydrogen-bonded end groups; (b) with external F2 hydrogen-bonded end groups.

to other chain ends and others folded into the interior of the lamella. With time these defects are removed as chains move axially (as well as laterally) to form the more regular IF structures.

Morphologies in the Final State. What is apparent from these studies, as was found earlier,^{14,18} is that well-crystallized E chain crystals always contain F2 chains mixed within the lamella. This is supported by the SAXS data¹⁴ and by the observation of a single DSC melting peak.^{14,24} Even prolonged annealing at high temperature does not remove the F2 LAM peak.¹⁴

While we previously proposed a feasible structure that could account for such a mixed crystal¹⁴ (see Figure 7a), it is clear that this is not the only, or even the most likely, possibility. In this structure, axial chain mobility could still convert the F2 to E chains. (In fact, the progressive NIF stem lengthening evident in some crystallizations may be evidence for such a process.) The persistence of F2 chains suggests that the structure of Figure 7b should be seriously considered. In such a case, the folded chains are indeed trapped in this configuration, both by the interior folds and by hydrogen bonding in the surface layers. This may be an unavoidable consequence of the crystallization process.

Conclusions

In-situ Raman LAM observations during crystallization from the melt at various temperatures have provided insights into the initial morphologies in a PEO 3000 fraction and how these structures change with time. It is clear that, although integer fold structures eventually develop, the initial lamellae consist of well-defined non-integer-fold chain stems. Their increasing length with temperature of crystallization suggests that these structures are kinetically determined. The NIF-to-IF conversion is clearly a solid-state transformation, and the development of extended chains may proceed through once-folded structures. In any case, the final lamellae always contain once-folded chains, probably trapped in morphologies that cannot transform into the extended form. The LAM studies are uniquely suited to deriving some of these conclusions.

Acknowledgment. This research was supported by NSF Grant DMR-9110353. We wish to thank Professor S. Z. D. Cheng for providing the MPEO sample.

References and Notes

- (1) Keller, A. *Philos. Mag.* **1957**, *8*, 1171.
- (2) Keller, A. *Pure Appl. Chem.* **1992**, *64*, 193.
- (3) Arlie, J. P.; Spegt, P.; Skoulios, A. *Makromol. Chem.* **1967**, *104*, 212.
- (4) Spegt, P. *Makromol. Chem.* **1970**, *139*, 139.
- (5) Kovacs, A. J.; Gonthier, A.; Straupe, C. *J. Polym. Sci., Polym. Symp.* **1975**, *50*, 283.
- (6) Buckley, C. P.; Kovacs, A. J. *Kolloid Z. Z. Polym.* **1976**, *254*, 695.
- (7) Mizushima, S.; Simanouti, T. *J. Am. Chem. Soc.* **1949**, *71*, 1320.
- (8) Strobl, G. R.; Eckel, R. *J. Polym. Sci., Polym. Phys. Ed.* **1976**, *14*, 913.
- (9) Hsu, S. L.; Krimm, S. *J. Appl. Phys.* **1976**, *47*, 4265.
- (10) Palmö, K.; Krimm, S. *J. Polym. Sci., Polym. Phys. Ed.* **1996**, *34*, 37.
- (11) Hartley, A.; Leung, Y. K.; Booth, C.; Shepherd, I. W. *Polymer* **1976**, *17*, 355.
- (12) Song, K.; Krimm, S. *J. Polym. Sci., Polym. Phys. Ed.* **1990**, *28*, 35.
- (13) Song, K.; Krimm, S. *J. Polym. Sci., Polym. Phys. Ed.* **1990**, *28*, 51.
- (14) Song, K.; Krimm, S. *Macromolecules* **1990**, *23*, 1946.
- (15) Rabolt, J. F. *CRC Crit. Rev. Solid State Mater. Sci.* **1985**, *12*, 165.
- (16) Folkes, M. J.; Keller, A.; Stejny, J.; Goggin, P. L.; Fraser, G. V.; Hendra, P. J. *Colloid Polym. Sci.* **1975**, *253*, 354.
- (17) Kim, I.; Krimm, S. *Macromolecules* **1994**, *27*, 5232.
- (18) Song, K.; Krimm, S. *Macromolecules* **1989**, *22*, 1504.
- (19) Cheng, S. Z. D.; Chen, J.; Wu, S.; Zhang, A.; Yandrasits, M. A.; Zhou, Q.; Quirk, R.; Habenschuss, A.; Zschack, P. R. In *Crystallization of Polymers*; Kluwer Academic Press: Dordrecht, 1993 and references therein.
- (20) Takahashi, Y.; Tadokoro, H. *Macromolecules* **1973**, *6*, 672.
- (21) Butcher, R. J.; Willetts, D. V.; Jones, W. J. *Proc. R. Soc. London* **1971**, *A324*, 231.
- (22) Placzek, G. *Marx's Handb. Radiol.* **1934**, *6*, 209.
- (23) Snyder, R. G.; Krause, S. J.; Scherer, J. R. *J. Polym. Sci., Polym. Phys. Ed.* **1978**, *16*, 1593.
- (24) Kim, I. Ph.D. Thesis, University of Michigan, 1995.
- (25) Schaufele, R. F.; Shimanouchi, T. *J. Chem. Phys.* **1967**, *47*, 3605.
- (26) Viras, K.; Teo, H. H.; Marshall, A.; Domszy, R. C.; King, T. A.; Booth, C. *J. Polym. Sci., Polym. Phys. Ed.* **1983**, *21*, 919.
- (27) Snyder, R. G.; Strauss, H. L.; Alamo, R.; Mandelkern, L. *J. Chem. Phys.* **1994**, *100*, 5422.
- (28) Cheng, S. Z. D.; Wu, S. S.; Chen, J.; Zhuo, Q.; Quirk, R. P.; von Meerwall, E. D.; Hsiao, B. S.; Habenschuss, A.; Zschack, P. R. *Macromolecules* **1993**, *26*, 5105.
- (29) Rabolt, J. F.; Johnson, K. W.; Zitter, R. N. *J. Chem. Phys.* **1974**, *61*, 504.
- (30) Cheng, S. Z. D.; Zhang, A.; Chen, J.; Heberer, D. P. *J. Polym. Sci., Polym. Phys. Ed.* **1991**, *29*, 287.
- (31) Hoffman, J. D. *Macromolecules* **1986**, *19*, 1124.
- (32) Ungar, G.; Keller, A. *Polymer* **1986**, *27*, 1835.

MA960331P